the actual rate ratio for *trans*-cyclooctene to *cis*-cyclooctene would be 200–1200, closer to what might be expected for electron transfer.

Therefore, although questions remain, the electron-transfer-carbocation mechanism appears to best explain the epoxidations of reactive alkenes.

Acknowledgment. We are grateful to the National Science Foundation (Grant CHE 84-20612) for support of this research and to Paul Maffuid for some initial syntheses.

(11) We have recently observed a small amount of cyclohexene-4-carboxaldehyde during catalyzed epoxidation of norbornene,[10b] indicating some skeletal rearrangement in that epoxidation.

High-Resolution ^{14}N Overtone Spectroscopy: An Approach to Natural Abundance Nitrogen NMR of Oriented and Polycrystalline Systems

R. Tycko and S. J. Opella*

Department of Chemistry, University of Pennsylvania Philadelphia, Pennsylvania 19104
Smith, Kline and French Laboratories Philadelphia, Pennsylvania 19101
Received October 15, 1985

In this paper, we present a novel approach to nitrogen NMR spectroscopy of both oriented and polycrystalline samples. The method employs the direct excitation and detection of ^{14}N overtone NMR transitions at approximately twice the ^{14}N Larmor frequency.[1]

New approaches to nitrogen NMR are needed both because of the chemical and biochemical importance of nitrogen and because of the limitations of current methods. In the solid state, ^{15}N NMR typically requires isotopic labeling to achieve sufficient sensitivity.[2-5] Through cross-polarization,[6] good sensitivity is achieved in ^{14}N NMR of single crystals. The large quadrupole interactions of ^{14}N nuclei provide high resolution in single-crystal spectra but at the expense of a spectral width of several megahertz.[7-16] Since the experimentally observable spectral range is only about 200 kHz, it is impossible to acquire a complete spectrum without repeated retuning of the spectrometer. ^{14}N powder pattern spectra have only been obtained with indirect detection[17] or when the quadrupole couplings are unusually small.[18,19] Large quadrupole couplings also limit the applicability of double-quantum[20-24] and zero-field[25-27] NMR techniques. For these reasons, we became interested in the insightful proposal by Bloom,[1a] and the experimental demonstration by Legros and Bloom,[1b] that ^{14}N overtone NMR transitions can be directly excited and detected in the solid state.

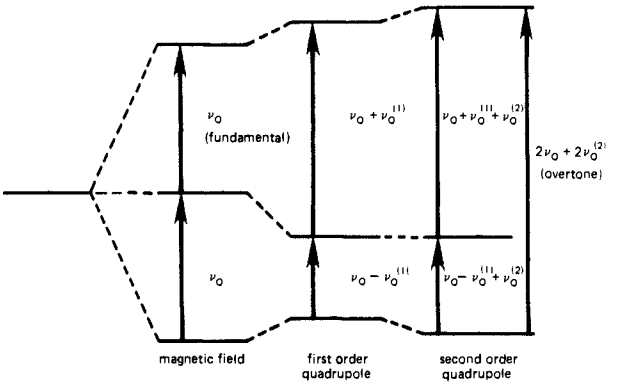

Figure 1. Spin energy level diagrams for ^{14}N NMR. In a large static magnetic field fundamental transitions at the Larmor frequency ν_0 (18.06 MHz in a 5.87-T field) are observed. The first-order effect of a quadrupole coupling in the solid state is to split the fundamental spectrum into a doublet, with a splitting of $2\nu_Q^{(1)}$ (up to 4.5 MHz with $e^2qQ/h = 3.0$ MHz). For large quadrupole couplings, a second-order shift $\nu_Q^{(2)}$ (up to approximately 50 kHz) is observed in the fundamental spectrum. Overtone transitions at $2\nu_0 + 2\nu_Q^{(2)}$ become allowed and can be directly detected by pulsed NMR.

The essential physical aspects of ^{14}N NMR are summarized in Figure 1. In an applied magnetic field, there are three spin energy levels separated by $h\nu_0$. Since only transitions at the Larmor frequency ν_0, i.e., the fundamental transitions, are allowed by dipole selection rules, a single resonance is observed. In solids and oriented systems, the quadrupole interaction effectively shifts the middle energy level with respect to the others by $\nu_Q^{(1)}$. When the quadrupole coupling constant e^2qQ/h is much smaller than ν_0, the fundamental spectrum becomes a doublet centered at ν_0 with a splitting of $2\nu_Q^{(1)}$. As e^2qQ/h becomes larger, second-order effects appear. One second-order effect is to shift the lowest energy level down and the highest energy level up by the second-order shift $\nu_Q^{(2)}$. The other second order effect, which is crucial for overtone NMR, is to make transitions between the lowest and highest energy levels, i.e., the overtone transitions, weakly allowed. Thus, a single resonance can be observed at $2\nu_0 + 2\nu_Q^{(2)}$, or approximately twice the ^{14}N Larmor frequency. Since the overtone frequency is only affected by $\nu_Q^{(2)}$, the total width of an overtone spectrum is less than that of a fundamental spectrum by a factor of approximately $8h\nu_0/e^2qQ$ (45 for the example shown here).

Figure 2 contains the first examples of high-resolution ^{14}N overtone NMR spectra obtained with proton decoupling and cross-polarization, illustrating the resolution and sensitivity of the technique. The two resonance lines in each spectrum arise from two inequivalent molecules in the unit cell of the 50-mg *N*-acetylvaline crystal. The 200-Hz line widths are approximately 10 times less than the corresponding fundamental line widths.[8] The comparison of Figure 2, parts A and B, demonstrates the signal enhancement resulting from cross-polarization using a

* Address correspondence to this author at the University of Pennsylvania.

(1) (a) Bloom, M., private communication. (b) Legros, M. M.Sc. Thesis, University of British Columbia, 1984.
(2) Cross, T. A.; DiVerdi, J. A.; Opella, S. J. *J. Am. Chem. Soc.* **1982**, *104*, 1759–1761.
(3) Cross, T. A.; Opella, S. J. *J. Mol. Biol.* **1985**, *182*, 367–381.
(4) Huang, T.-H.; Bachovchin, W. W.; Griffin, R. G.; Dobson, C. M. *Biochemistry* **1984**, *23*, 5933–5937.
(5) Gibby, M. G.; Griffin, R. G.; Pines, A.; Waugh, J. S. *Chem. Phys. Lett.* **1972**, *17*, 80–81.
(6) Pines, A.; Gibby, M. G.; Waugh, J. S. *J. Chem. Phys.* **1972**, *56*, 1776–1777.
(7) Wolff, E. K.; Griffin, R. G.; Watson, C. *J. Chem. Phys.* **1977**, *66*, 5433–5438.
(8) Stark, R. E.; Haberkorn, R. A.; Griffin, R. G. *J. Chem. Phys.* **1978**, *68*, 1996–1997.
(9) Griffin, R. G.; Bodenhausen, G.; Haberkorn, R. A.; Huang, T. H.; Munowitz, M.; Osredkar, R.; Ruben, D. J.; Stark, R. E.; van Willigen, H. *Philos. Trans. R. Soc. London, A* **1981**, *299*, 547–563.
(10) Haberkorn, R. A.; Stark, R. E.; van Willigen, H.; Griffin, R. G. *J. Am. Chem. Soc.* **1981**, *103*, 2534–2539.
(11) Naito, A.; Ganapathy, S.; Raghunathan, P.; McDowell, C. *J. Chem. Phys.* **1983**, *79*, 4173–4182.
(12) Naito, A.; Barker, P.; McDowell, C. *J. Chem. Phys.* **1984**, *81*, 1583–1591.
(13) Naito, A.; McDowell, C. *J. Chem. Phys.* **1984**, *81*, 4795–48034.
(14) Suter, D.; Ernst. R. R. *Phys. Rev. B* **1982**, *25*, 6038–6041.
(15) Blinc, R.; Mali, M.; Osredkar, R.; Prelesnik, A.; Zupancic, I. *J. Chem. Phys.* **1971**, *55*, 4843–4848.
(16) Blinc, R.; Mali, M.; Osredkar, R.; Prelesnik, A.; Zupancic, I. *Chem. Phys. Lett.* **1971**, *9*, 85–87.
(17) Schnur, G.; Kimmich, R.; Winter, F. *J. Magn. Reson.* **1986**, *66*, 295–306.
(18) Pratum, T. K.; Klein, M. P. *J. magn. Reson.* **1983**, *53*, 473–485.
(19) Pratum, T. K.; Klein, M. P. *J. Magn. Reson.* **1983**, *55*, 421–437.
(20) Vega, S.; Shattuck, T. W.; Pines, A. *Phys. Rev. Lett.* **1976**, *37*, 43–46.
(21) Vega, S.; Pines, A. *J. Chem. Phys.* **1977**, *66*, 5624–5644.
(22) Vega, S.; Shattuck, T. W.; Pines, A. *Phys. Rev. A* **1980**, *22*, 638–661.
(23) Brunner, P.; Reinhold, M.; Ernst, R. R. *J. Chem. Phys.* **1980**, *73*, 1086–1094.
(24) Reinhold, M.; Brunner, P.; Ernst, R. R. *J. Chem. Phys.* **1981**, *74*, 184–188.
(25) Weitekamp, D. P.; Bielecki, A.; Zax, D.; Zilm, K.; Pines, A. *Phys. Rev. Lett.* **1983**, *50*, 1807–1810.
(26) Millar, J. M.; Thayer, A. M.; Bielecki, A.; Zax, D. B.; Pines, A. *J. Chem. Phys.* **1985**, *83*, 934–938.
(27) Zax, D. B.; Bielecki, A.; Zilm, K. W.; Pines, A.; Weitekamp, D. P. *J. Chem. Phys.* **1985**, *83*, 4877–4905.

0002-7863/86/1508-3531$01.50/0

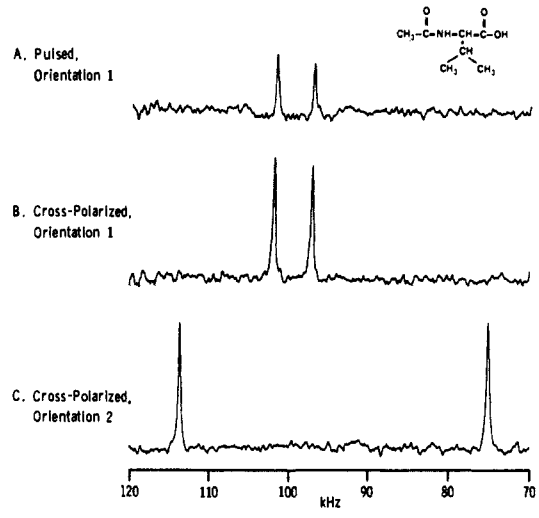

Figure 2. Proton-decoupled ^{14}N overtone NMR spectra of a single crystal of *N*-acetylvaline. (A) Directly pulsed spectrum, using a 30-ms nitrogen overtone if pulse at 36.212 MHz (ν_0 = 18.059 MHz); 1024 transients with a 1-s recycle delay. The two lines arise from two inequivalent molecules in the unit cell. The frequency scale is relative to $2\nu_0$ = 36.118 MHz. (B) Spectrum obtained with cross-polarization from proton dipolar order, demonstrating signal enhancement 1024 transients with a 1-s recycle delay. (C) Spectrum obtained with cross-polarization after an arbitrary 10° rotation of the crystal, illustrating the sensitivity of the overtone frequencies to orientation.

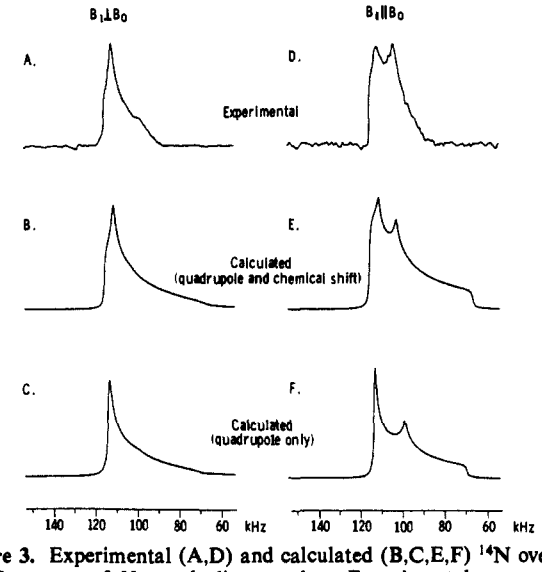

Figure 3. Experimental (A,D) and calculated (B,C,E,F) ^{14}N overtone NMR spectra of *N*-acetylvaline powder. Experimental spectra were obtained with proton decoupling and cross-polarization. The overtone if field B_1 was applied perpendicular to the static field B_0 in (A)–(C) and parallel to B_0 in (D)–(F). Each experimental spectrum is the result of approximately 30 000 scans with a carrier frequency of 36.225 MHz. In the calculated spectra, the signal contribution of each crystallite orientation is weighted by the magnitude of the overtone transition moment at that orientation. In the experimental spectra, the intensities are determined by both the transition moment and the cross-polarization efficiency. Both second-order quadrupole shifts and chemical shifts were included in the calculations of (B) and (E); only second-order quadrupole shifts were considered in the calculations of (C) and (F).

Jeener–Broekaert sequence.[28] Figure 2C illustrates the sensitivity of the overtone frequencies to molecular orientation, primarily due to the orientational dependence of $\nu_Q^{(2)}$.

Figure 3 contains the first overtone NMR spectra of a polycrystalline sample. Spectra of a 230-mg powder sample of *N*-acetylvaline were obtained with two different double-resonance probe configurations. The spectrum in Figure 3A was obtained by using a double-tuned probe with a radiofrequency solenoid coil perpendicular to the static field B_0, which is the usual configuration in solid-state NMR. The spectrum in Figure 3D was obtained by using a probe with a solenoid coil *parallel to* B_0[1,29] for ^{14}N irradiation near $2\nu_0$ and a Helmholtz coil perpendicular to B_0 for proton irradiation. The fact that two sharp features appear in Figure 3D while only a single sharp feature appears in Figure 3A is a consequence of the different orientational dependences of the overtone transition moment in the two coil configurations.

The positions of the sharp features in Figure 3A,D are determined primarily by the values of e^2qQ/h and the quadrupole asymmetry parameter η. In addition, effects of chemical shift anisotropy (CSA) are apparent in the details of the shapes of the spectral features. Parts B and E of Figure 3 are calculated overtone powder patterns for the perpendicular and parallel coil configurations in which the values e^2qQ/h = 3.24 MHz and η = 0.27 were used, along with an axially symmetric CSA tensor characterized by $\sigma_\parallel = -114$ ppm and $\sigma_\perp = 57$ ppm. The values of e^2qQ/h and η were determined from the experimental spectra, and are in good agreement with previously reported values.[8,30] The values of $\sigma_\parallel$ and $\sigma_\perp$ were taken from ^{15}N NMR studies of peptides and proteins.[31,32] In Figure 3B,E the principal axis of the CSA tensor was taken to be aligned with the x axis of the quadrupole tensor. Parts C and F of Figure 3 are powder patterns calculated without including CSA effects, showing that the quadrupole interaction accounts for the principal features of the experimental spectra.

Acknowledgment. We thank M. Bloom for communicating his results prior to publication and P. Stewart for the loan of the *N*-acetylvaline crystal. This research was supported in parts by grants (GM-24266 and GM-29754) from the N.I.H. R.T. acknowledges support from a Damon Runyon–Walter Winchell Cancer Fund Fellowship, DRG-891.

Registry No. *N*-Acetylvaline, 96-81-1.

(28) Jeener, J.; Broekaert, P. *Phys. Rev.* **1967**, *157*, 232–240.

(29) (a) Analogous effects have been exploited in EPR studies of optically excited triplet states. (b) van der Waals, J. H.; de Groot, M. S. *Mol. Phys.* **1959**, *2*, 333–340. (c) de Groot, M. S.; van der Waals, J. H. *Mol. Phys.* **1960**, *3*, 190–200.

(30) Sadiq, G. F.; Greenbaum, S. G.; Bray, P. J. *Org. Magn. Reson.* **1981**, *17*, 191–193.

(31) Harbison, G. S.; Jelinski, L. W.; Stark, R. E.; Torchia, D. A.; Herzfeld, J.; Griffin, R. G. *J. Magn. Reson.* **1984**, *60*, 79–82.

(32) Cross, T. A.; Opella, S. J. *J. Mol. Biol.* **1985**, *182*, 367–381.

Catalytic Decomposition of 2-Propanol on Single-Crystal Surfaces of ZnO

P. Berlowitz and H. H. Kung*

Chemical Engineering Department and the Ipatieff Laboratory, Northwestern University Evanston, Illinois 60201

Received December 30, 1985

The concept of Bourdart[1] of structure sensitivity in heterogeneous catalytic reactions suggests that the kinetics and the mechanism of a reaction may depend on the surface structure and the crystalline size of the catalyst. Investigation of the surface structural effect is made possible by surface science techniques using single-crystal samples.[2-4] It is interesting to note that all the examples reported have been on metal surfaces. We report here the first example of surface structural effect on single-crystal surfaces of an oxide, specifically zinc oxide.

(1) Boudart, M. *Adv. Catal.* **1969**, *20*, 153.

(2) Blakely, D. W.; Somorjai, G. A. *J. Catal.* **1976**, *42*, 181.

(3) Gale, G. J.; Salmeron, M.; Somorjai, G. A. *Phys. Rev. Lett.* **1977**, *38*, 1027; *J. Chem. Phys.* **1977**, *67*, 5324.

(4) Somorjai, G. A. *Chemistry in Two Dimensions, Surfaces*, Cornell University Press: New York, 1981.

0002-7863/86/1508-3532$01.50/0